Proceedings of the 16th International Conference on Industrial Engineering and Operations Management
Ankara, Türkiye, June 23-25, 2026

Proceedings of the International Conference on Industrial Engineering and Operations Management

Publisher: IEOM Society International, USA DOI: 10.46254/AN16.20260023
Published: June 23, 2026

Bi-Level Optimization for Energy-Efficient Heater Placement in Manufacturing Systems

Aybüke Ekşi, Milad Elyasi and Okan Örsan Özener
Industrial Engineering Department
Özyeğin University, Istanbul, Turkey
aybuke.eksi@ozu.edu.tr, milad.elyasi@ozyegin.edu.tr, orsan.ozener@ozyegin.edu.tr

Altuğ Melik Başol
Mechanical Engineering Department
Özyeğin University, Istanbul, Turkey
altug.basol@ozyegin.edu.tr

Abstract

This study proposes a bi-level optimization framework for heater placement in 2D manufacturing systems, such as oven configurations, with a focus on achieving uniform heat distribution and energy efficiency. The first level minimizes the maximum absolute deviation of view factors from their average, ensuring uniform thermal management across surface segments. The second level minimizes the number of active heaters while maintaining the thermal uniformity achieved in the first level, promoting energy savings. Computational results across multiple scenarios demonstrate that the framework effectively reduces heater usage by an average of 6% while preserving heat uniformity, using only 45% of the total heater capacity in some cases. By leveraging view factor-based heat transfer models, inverse heat conduction analysis, and bi-level optimization, this work aligns with key Industry 4.0 principles, particularly smart manufacturing and energy-efficient production. The proposed framework offers a data-driven approach to heater placement, enabling intelligent thermal management through computational methods. Its ability to reduce energy consumption while maintaining thermal uniformity supports sustainable manufacturing and creates opportunities for integration with real-time monitoring and process optimization systems.

Keywords
Bi-level optimization, manufacturing system design/reconfiguration, optimization and control, sustainable manufacturing, Industry 4.0.

1. Introduction
In the context of Industry 4.0, the integration of advanced computational methods and optimization techniques into manufacturing processes is essential for achieving higher efficiency, sustainability, and product quality. Modern manufacturing systems face increasing demands for energy-efficient operations and precise control over production environments. One critical aspect of this is thermal management, particularly in systems where uniform heat distribution is vital, such as oven configurations used in food production, materials processing, and electronics manufacturing. Inefficient heater placement often leads to uneven heat distribution, resulting in energy waste, inconsistent product quality, and increased operational costs. These challenges necessitate innovative approaches to heater design that maximize thermal efficiency while minimizing energy consumption.

Recent advances in heat transfer modeling and optimization techniques provide promising pathways for addressing the challenges of thermal system design in manufacturing. Inverse Heat Conduction Problems (IHCPs) serve as a foundational tool in heater optimization by enabling the estimation of unknown thermal properties or boundary conditions through data-driven analysis. However, traditional solution methods often struggle in complex industrial environments. To overcome these challenges, advanced numerical techniques such as finite element and finite difference methods have been widely adopted to stabilize and solve IHCPs effectively (Jarny and Abou Khachfe, 2000). Studies such as Liu (2008) and Raudensky et al. (1995) demonstrate the efficacy of genetic algorithms in optimizing heater placements in multidimensional configurations, ensuring precise parameter estimation and consistent temperature control. Additionally, optimization methodologies like response surface modeling integrated with finite element simulations (Cheng et al., 2009) and sequential metamodeling approaches (Cheng et al., 2010) have proven successful in refining heat source placements and improving computational efficiency.

Despite these advances, many existing techniques focus primarily on optimizing heat distribution without explicitly addressing energy efficiency. Recent research has explored transient optimization techniques (Daun et al., 2004) to dynamically adjust heater settings over time, striking a balance between uniform heat distribution and energy savings. Furthermore, experimental optimization of heating elements has improved thermal performance while reducing energy costs (Hachchadi et al., 2023). However, simultaneous optimization of heater configurations to achieve both thermal uniformity and energy efficiency in manufacturing systems remains a significant challenge. Balancing these two often-conflicting goals, including uniform heating and minimal energy use, requires a more nuanced and integrated modeling approach.

Unlike prior studies that rely on heuristic adjustments or purely experimental approaches, this study presents a bi-level optimization framework tailored for heater placement in 2D manufacturing systems, with a specific focus on oven configurations. The framework ensures uniform heat distribution while minimizing energy consumption, directly contributing to sustainable manufacturing practices and energy management—key pillars of modern industrial innovation. The first level of optimization minimizes the maximum absolute deviation of view factors from their average, ensuring uniform thermal management across surface segments. The second level minimizes the number of active heaters while preserving the thermal uniformity achieved in the first level, thereby optimizing energy usage. By employing advanced mathematical optimization and computational intelligence, this approach supports the digitalization of manufacturing design processes in line with Industry 4.0 objectives, offering a scalable solution for energy-efficient production with potential societal benefits such as reduced environmental impact and improved product quality.

2. Problem Definition

The optimization of heater placement in 2D systems, such as the oven configuration, involves determining the optimal locations and activation states of the heaters while ensuring uniform heat distribution across the surface. This study applies heat transfer models and thermal design optimization to refine heater placement. Key parameters include source and surface dimensions, heater area, and heater-to-surface distance.

2.1 View Factors and Its Formulation

Key inputs for view factor calculations include surface dimensions, the count of heater resources, and the heater-to-surface distance. To quantify the heat received by each surface element from each heater element, a View Factor Matrix *F (i, j)* is used. This matrix represents the proportion of radiative heat energy leaving a surface element *i* that reaches a heater element *j*, based on their relative positions, orientations, and distances. The view factor calculation directly accounts for these geometric relationships, determining the fraction of radiation energy transferred between surfaces. As a crucial parameter in heat transfer modeling, it ensures that heat distribution follows precise constraints, ensuring that the desired temperature profiles are achieved.

2.2 Geometric and Mathematical Formulation of the View Factor

As shown in Figure 1, the view factor depends on several parameters:

- dA_1 and dA_2: Differential areas on the surface and heater, respectively.
- θ_1 and θ_2: Angles between the surface normals and the distance line r connecting the elements.
- *r*: Distance of the line connecting the surface and heater elements.

The formulation of the view factor for infinitesimal surface elements is given by:

$$F_{dA_1 \to dA_2} = \frac{\dot{Q}_{dA_1 \to dA_2}}{\dot{Q}_{dA_1 \to hemisphere}} = \frac{\cos(\theta_1)\cos(\theta_2)dA_2}{\pi r^2} \qquad (1)$$

For finite geometries, this can be expressed in terms of specific cells:

$$F_{i\to j} = \frac{\cos(\theta_i)\cos(\theta_j)A_{cell,j}}{\pi r^2{}_{i\to j}} \tag{2}$$

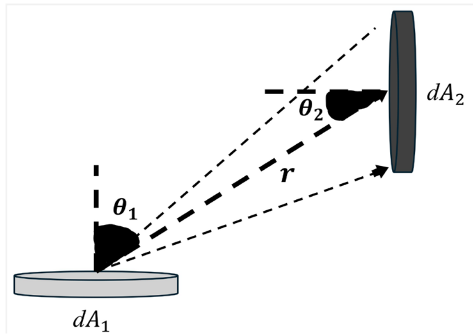

Figure 1: Illustration of the view factor F (i, j) between a surface element dA_1 and a heater element dA_2 showing the geometric parameters θ_1, θ_2 and r that influence the calculation.

2.3 Simplifications of the View Factor Formulation

The geometric illustration of the calculation of the view factor is shown in Figure 2.

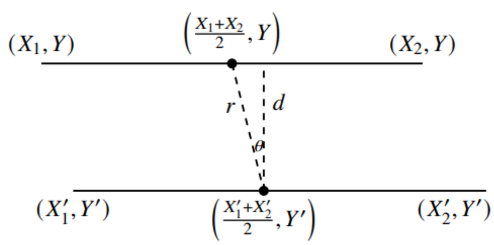

Figure 2: Geometric illustration of the view factor calculation.

The angle θ in the view factor calculation is determined as:

$$\theta = \arccos\left(\frac{Y-Y'}{r}\right) \tag{3}$$

For specific configurations, the view factor can be expressed as:

$$F_{i\to j} = \frac{(\frac{(Y-Y')}{r})^2 A}{\pi r^2} \tag{4}$$

where, $A_{cell,j} = A$ represents the area of the resource segment (grid).

Further simplifications lead to:

$$F_{i\to j} = \frac{d^2 A}{\pi r^4} \tag{5}$$

As the final step, the view factor, used as a parameter in the represented model, is expressed as:

$$F_{(i,i')\to(j,j')} = \frac{d^2 A}{\pi r^4_{ii'jj'}} \tag{6}$$

These formulations emphasize the geometric and radiative dependencies of the view factor, ensuring accurate computation in practical heat transfer applications. According to these, our study utilizes two optimization models as solution approach.

3. Solution Method: Optimization Framework

The optimization framework consists of a bi-level process aimed at achieving thermal uniformity and energy efficiency:

First Level: The initial optimization model minimizes the maximum absolute deviation of the view factors to ensure a uniform heat distribution across the surface.

Second Level: Using the results of the first model, the second optimization model minimizes the number of active heaters while preserving the thermal uniformity established earlier.

The mathematical models incorporate geometric and radiative dependencies, leveraging calculated view factors based on the relative positioning of heaters and surface segments. The calculated threshold is based on the expected output, which corresponds to approximately 45% of the total capacity when all possible heaters in a heating system are activated. This rate reflects a typical average operating level of total heating capacity used for temperature maintenance in certain industrial ovens. This value serves as the baseline for the average view factor and is used as the threshold (T) in both models. In the second model, a tolerance parameter is included to balance thermal performance with energy efficiency. Both models are solved sequentially using Mixed-Integer Programming (MIP) with a commercial solver Gurobi Optimizer 10.0.3. On average, the first model required approximately 0.15 seconds to reach an optimal solution, while the second model solved in approximately 0.03 seconds, demonstrating the practicality of the approaches. Table 1 presents the sets, parameters, and decision variables used in the optimization models.

Table 1: Nomenclature for the Problem

Sets	
I	set of resource segments ($\{0, 1, \ldots, n\}$) – indexed by (i, i')
J	set of surface segments ($\{0, 1, \ldots, m\}$) – indexed by (j, j')
Parameters	
T	threshold for the average view factor
Z^*	optimal solution of the first model (second model)
k	tolerance coefficient: **0.2** (second model)
$F_{(i,i'),(j,j')}$	view factor amount
Decision variables	
$X_{(i,i')}$	1, if the segment of the resource (i, i') is opened (used); 0, otherwise
$Y_{(j,j')}$	Amount of view factor in the segment of the surface (j, j')
Y_{avg}	Average value of the $Y_{(j,j')}$
Δ	Amount of absolute deviation between view factor

3.1 Level 1 Optimization Model

In the following, we present the mathematical formulation of the first optimization model, which focuses on minimizing the maximum absolute deviation between the view factor and the average of them in the surface segments to achieve uniform heat distribution across the surface while maintaining thermal efficiency.

$$\min \quad \Delta \tag{7}$$

$$Y_{(j,j')} = \sum_{(i,i')\in I} F_{(i,i'),(j,j')} X_{(i,i')} \qquad \forall (j,j') \in J \tag{8}$$

$$\sum_{(j,j')\in J} Y_{(j,j')}/|J| = Y_{\text{avg}} \tag{9}$$

$$Y_{\text{avg}} \geq T \tag{10}$$

$$\Delta \geq Y_{(j,j')} - Y_{\text{avg}} \qquad \forall (j,j') \in J \tag{11}$$

$$\Delta \geq Y_{\text{avg}} - Y_{(j,j')} \qquad \forall (j,j') \in J \tag{12}$$

$$X_{(i,i')} \in \{0,1\} \qquad \forall (i,i') \in I \tag{13}$$

$$Y_{(j,j')} \geq 0 \qquad \forall (j,j') \in J \tag{14}$$

$$Y_{\text{avg}} \geq 0 \tag{15}$$

$$\Delta \geq 0 \tag{16}$$

The objective function (7) minimizes the maximum absolute deviation of view factors from their average, ensuring uniform heat distribution across all surface segments. Constraint (8) calculates the view factor for each surface segment as a function of the contribution from all active resource segments. The view factor is determined by parameters such as the geometric relationship between resource and surface segments and the binary activation variable. Constraint (9) enforces the calculation of the average view factor as the mean of all view factor values across the surface segments. Constraint (10) ensures that average view factor meets or exceeds a specified threshold, maintaining a minimum baseline of heat transfer. Constraints (11) and (12) linearize the absolute deviations of view factor amounts from average view factor by introducing the maximum deviation. The binary constraint (13) ensures that resource activation decisions are valid, taking either 0 or 1. Constraints (14-16) are the non-negativity constraints.

3.2 Level 2 Optimization Model

Optimization Model 2 builds upon the results obtained from Model 1. Specifically, the parameter Z^* represents the optimal solution obtained from Model 1, which is used as a benchmark to ensure a minimum level of maximum view factor across surface segments in Model 2. Thus, while Model 2 aims to minimize the number of active heaters to optimize energy consumption, it ensures that the thermal uniformity established in Model 1 is preserved within an allowable variability, thereby balancing efficiency and performance.

$$\min \quad \sum_{(i,i')\in I} X_{(i,i')} \tag{17}$$

$$\Delta \leq (1+k)Z^{*} \tag{18}$$

The objective function (17) minimizes the total number of active resources, promoting efficient use of resources while ensuring uniform heat distribution across all surface segments. Constraint (18) limits the maximum absolute deviation to a fraction of the optimal threshold deviation, controlling the allowable variability in heat distribution. The remaining constraints (19-27) follow the same structure as those defined in Model 3.1 (8-16).

4. Numerical Results

The experimental design encompasses three key scenarios to analyze the distribution of resources across a surface. Two resource-to-surface distances are considered, d = 10 and d = 15, to assess the impact of proximity on distribution efficiency. The presented design incorporates three distinct scenarios, as detailed in Table 2, each defined by the grid dimensions of the Resource Allocation Panel (RAP) and Heat Intensity Panel (HIP), each having the same number of resources (n) and surface points (m), with n = 100 and m = 100 counts:

- **Scenario 1:** The RAP and HIP have identical dimensions, specifically, 10 × 10 and 20 × 20. For both configurations, two resource-to-surface distances, (d = 10 and d = 15) are considered, with a balanced number of resource and surface points.
- **Scenario 2:** The RAP has larger dimensions than the HIP. Specifically, the RAP is 20 × 20 while the HIP remains 10 × 10, and the RAP is 25 × 25 while the HIP is 15 × 15. Similar configurations are implemented, analyzing two distances (d = 10 and d = 15), with the same number of resource and surface grid points.

- **Scenario 3:** The RAP is smaller than the HIP. The RAP is set to 10 × 10 while the HIP is 20 × 20, and in another configuration, the RAP is 15 × 15 while the HIP expands to 25 × 25. Again, both resource-to-surface distance setups (d = 10 and d = 15) are evaluated while maintaining a fixed number of grid points for resources and surfaces.

The computational results are visualized through figures, each comprising two panels:

1. **RAP:** This panel shows the binary decision variable $X_{(i,i')}$, where red cells represent active resources ($X_{(i,i')}$= 1) and white cells represent unused resources ($X_{(i,i')}$= 0). Strategic patterns, such as cross-shaped white regions, indicate optimal resource allocations to enhance energy efficiency and heat distribution.
2. **HIP:** This panel displays a heatmap of the continuous decision variable $Y_{(j,j')}$, representing view factor intensity. A gradient from light red (low intensity) to dark red (high intensity) highlights spatial variations, emphasizing regions of higher thermal demand.

Table 2: Instance Table

Instance	Scenario	d	Grid Dimension of RAP	Grid Dimension of HIP	n	m
1	1	10	10x10	10x10	100	100
2			20x20	20x20		
3		15	10x10	10x10		
4			20x20	20x20		
5	2	10	20x20	10x10	100	100
6			25x25	15x15		
7		15	20x20	10x10		
8			25x25	15x15		
9	3	10	10x10	20x20	100	100
10			15x15	25x25		
11		15	10x10	20x20		
12			15x15	25x25		

The computational results for all instances and their respective scenarios are presented in comprehensive, horizontally aligned figures, consolidating the outputs of both models under varying resource-to-surface distances. Each scenario consists of four instances, with each instance displaying Model 1 results at the top and Model 2 results at the bottom. Additionally, each instance contains two visualization panels for both models: the first panel (RAP) illustrates the grid visualization, highlighting resource allocation patterns, while the second panel (HIP) presents the heatmap of view factor intensities. In each scenario, instances (a) and (b) represent the results for a resource-to-surface distance of 10, whereas instances (c) and (d) correspond to distance of 15. These structured visualizations provide a clear and comparative overview across all scenarios, demonstrating variations in resource distribution and heat intensity under different configurations. The summarized results are systematically incorporated into Figures 3, 4, and 5, ensuring clarity, consistency, and ease of interpretation by presenting the data in a well-organized and condensed format.

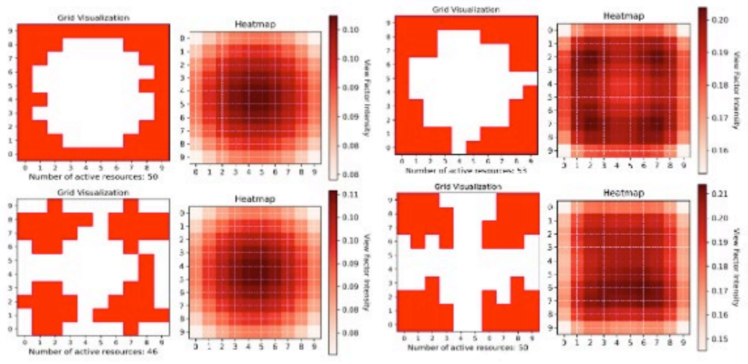

(a) Instance 1 (b) Instance 2

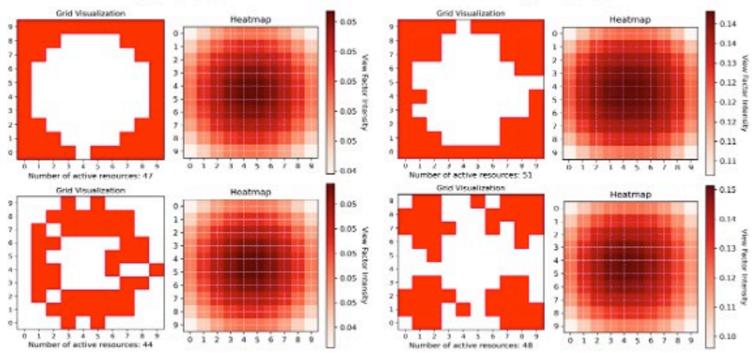

(c) Instance 3 (d) Instance 4

Figure 3: Consolidated Results for Scenario 1

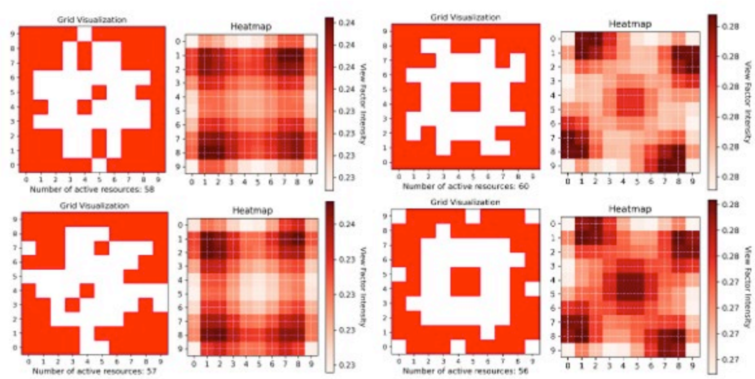

(a) Instance 5 (b) Instance 6

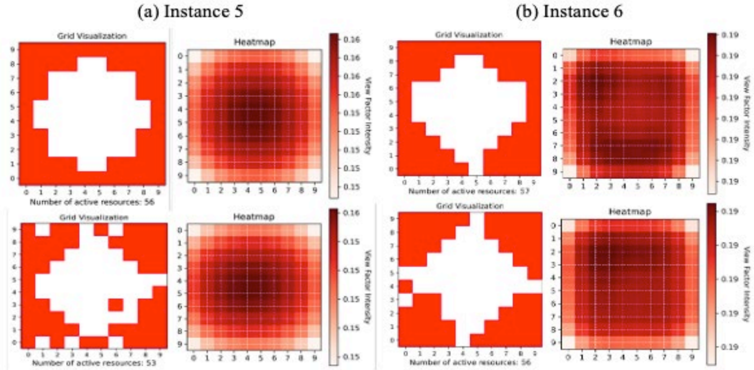

(c) Instance 7 (d) Instance 8

Figure 4: Consolidated Results for Scenario 2

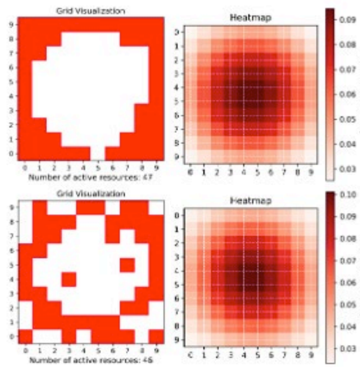

(a) Instance 9

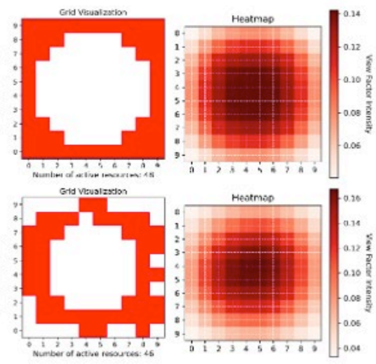

(b) Instance 10

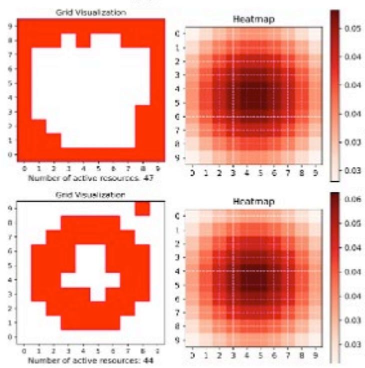

(c) Instance 11

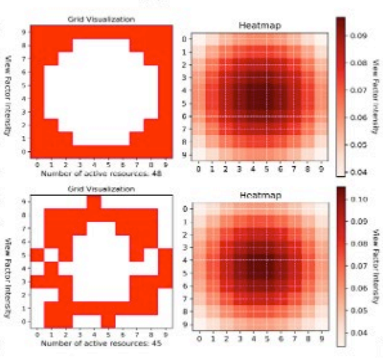

(d) Instance 12

Figure 5: Consolidated Results for Scenario 3

4.1 General Discussion

The numerical results highlight the trade-offs between thermal uniformity and energy efficiency in the proposed optimization framework. The first level, applied in Model 1, prioritizes uniform heat distribution by minimizing the absolute deviation of view factors, ensuring consistent heating across the surface. The second level, implemented in Model 2, reduces the number of active heaters while maintaining thermal uniformity, thereby optimizing energy consumption.

The impact of resource-to-surface distance ($d = 10$ vs. $d = 15$) is evident in both levels. At shorter distances, uniform heating is easier to achieve, whereas at greater distances, ensuring thermal uniformity requires a more strategic balance between resource allocation and heat intensity. In such cases, Model 2 effectively optimizes energy consumption by using fewer resources while preserving an acceptable level of uniformity, as indicated by the number of active resources in the grid visualization figures.

In Table 3, we present a comparative analysis of Model 1 and Model 2 across multiple instances and scenarios, focusing on their efficiency in resource allocation, heat distribution uniformity, and computational performance. The table summarizes key performance metrics, including heat distribution deviation (Δ), the number of active resources, solution optimality, and computation time. This allows for a detailed evaluation of how each model adapts to different resource availability conditions. Scenario-specific results indicate that Model 1 excels when resources are abundant or balanced, ensuring uniform heating, whereas Model 2 is more effective in resource-limited cases by strategically concentrating heating to maintain efficiency. As shown in Table 3, Model 1 generally activates more resources and achieves optimality more consistently, but it occasionally suffers from significantly higher solution times, especially in Instance 11 of Scenario 3. Model 2, on the other hand, is more resource-efficient, promoting energy efficiency, and solves most instances faster, but it struggles with optimality in cases like Instance 5 and 6 of Scenario 2. The trade-off between computational efficiency and solution quality is evident, suggesting that both models are valuable and applicable to real-world heating system configurations.

Table 3: Performance Comparison of Model 1 and Model 2 Across All Instances

	Scenario 1							
	Instance 1		Instance 2		Instance 3		Instance 4	
	Model 1	Model 2	Model 1	Model 2	Model 1	Model 2	Model 1	Model 2
Δ	0.017	0.020	0.036	0.043	0.006	0.020	0.027	0.032
Num. of Active Resources	50	46	53	50	48	44	51	48
Optimality Gap	0.000%	0.000%	0.000%	0.000%	0.000%	0.000%	0.000%	0.000%
Solution Time (in seconds)	3.472	0.388	1.642	0.157	0.110	0.220	1.836	1.341
	Scenario 2							
	Instance 5		Instance 6		Instance 7		Instance 8	
	Model 1	Model 2	Model 1	Model 2	Model 1	Model 2	Model 1	Model 2
Δ	0.001	0.020	0.002	0.002	0.006	0.007	0.006	0.007
Num. of Active Resources	58	57	60	56	56	53	57	56
Optimality Gap	0.000%	1.754%	0.000%	0.000%	0.000%	0.000%	0.000%	0.000%
Solution Time (in seconds)	1332.563	7203.465	1038.950	5301.22	2.413	2.018	1.272	0.879
	Scenario 3							
	Instance 9		Instance 10		Instance 11		Instance 12	
	Model 1	Model 2	Model 1	Model 2	Model 1	Model 2	Model 1	Model 2
Δ	0.036	0.043	0.058	0.069	0.015	0.018	0.031	0.037
Num. of Active Resources	47	46	48	46	47	44	48	45
Optimality Gap	0.000%	0.000%	0.000%	0.000%	1.004%	0.000%	0.000%	0.000%
Solution Time (in seconds)	0.805	0.359	0.236	0.173	7268.289	0.114	0.110	0.157

For instance, in Instance 12 of Scenario 3, Model 1 emphasizes uniformity, achieving a heat distribution deviation (Δ) of 0.0308 by allocating 48 resources evenly across the surface. Conversely, Model 2 adopts a more energy-efficient approach, allowing a slight increase in deviation to 0.0370, while reducing the number of active resources from 48 to 45 based on the predefined threshold. This adjustment results in an approximate 6.25% reduction in active resources, demonstrating a trade-off between energy efficiency and uniformity.

By optimizing resource allocation in this manner, Model 2 effectively lowers operational energy costs while maintaining acceptable uniformity levels. These findings highlight the practical significance of dynamic resource management in energy-intensive systems. Future studies could further quantify these efficiency gains in terms of total energy savings (kWh) and cost reductions, providing deeper insights into the real-world applicability of the proposed framework.

Visual insights from the Resource Allocation Plots (RAP) and Heat Intensity Plots (HIP) confirm that Model 1 distributes heating evenly, while Model 2 concentrates heating where it is most effective. This structured optimization framework enhances both uniformity and efficiency, making it particularly valuable for industrial applications requiring precise thermal control and energy savings.

4.2 Validation

To validate the proposed bi-level optimization framework beyond internal model-to-model comparisons, we benchmark Model 2 against simple, yet meaningful baseline heater selection strategies constructed on the same discretized geometry and view factor matrix.

For each instance, we fix the number of active heaters in the baseline strategies to match the number selected by Model 2 (denoted by $p = \sum_{(i,i')\in I} X_{(i,i')}^{(M2)}$) ensuring a fair comparison under an equal "heater (energy) budget." This allows us to assess whether Model 2 achieves better thermal uniformity through structured optimization rather than arbitrary deactivation of heaters.

Given any candidate heater activation vector X, the induced view factor intensity on each surface segment is computed as

$$Y_{(j,j')}(X) = \sum_{(i,i')\in I} F_{(i,i'),(j,j')} X_{(i,i')},$$

with average $Y_{avg}(X) = \frac{1}{|J|}\sum_{(j,j')\in J} Y_{(j,j')}(X)$.

Uniformity is evaluated using the same maximum absolute deviation metric employed in Model 1:

$$\Delta(X) = \max_{(j,j')\in J} \left|Y_{(j,j')}(X) - Y_{\text{avg}}(X)\right|.$$

We consider the following baselines:

- **Uniform placement (Baseline A):** p heaters are selected in an evenly spaced deterministic pattern over the RAP grid to emulate a standard engineering "uniform layout" design.
- **Random selection (Baseline B):** p heaters are selected uniformly at random from the RAP grid. We perform R independent trials (here, R = 30) and report the mean and standard deviation of $\Delta(X)$.

We compare the deviation Δ obtained from Model 2 with that from Baseline A and Baseline B for one test instance randomly selected from each scenario. Table 4 summarizes the performance of these example results:

Table 4: Comparison of Thermal Deviation Across Strategies

Instance	p	$\Delta_{\text{Model 2}}$	$\Delta_{\text{Baseline A}}$	$\Delta_{\text{Baseline B}}$ (mean ± std)
Instance 3	44	0.020	0.0430	0.0250 ± 0.0024
Instance 7	53	0.007	0.0488	0.0285 ± 0.0019
Instance 12	45	0.037	0.0439	0.0254 ± 0.0027

The validation results demonstrate that Model 2 yields consistently superior heater activation patterns compared to both uniform and random baselines, even under identical heater budgets. In Instance 3, Model 2 reduces the thermal deviation Δ by over 50% relative to uniform placement and achieves better results than the average of the random strategy, indicating that the solution quality is not a product of chance. In Instance 7, the improvement is especially significant, with deviation reduced by more than 85% compared to the uniform baseline and over 75% relative to random selection. This reflects the model's ability to account for spatial structure in the view factor distribution.

Although the random baseline in Instance 12 shows a slightly lower mean deviation, Model 2 still performs better than the uniform layout and provides a consistent and replicable result. These findings confirm that the energy efficiency gains achieved by Model 2 result from geometry-aware optimization rather than arbitrary heater deactivation.

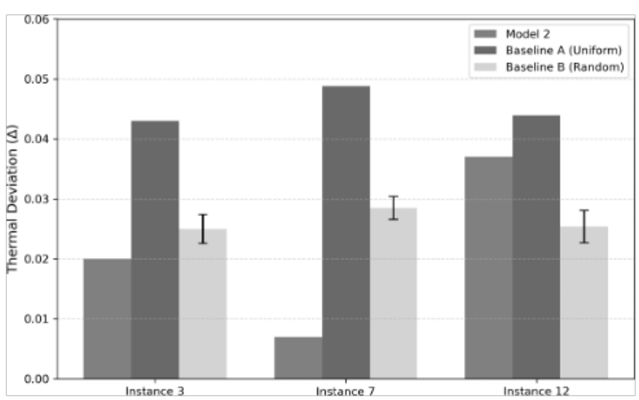

Figure 6: Comparison of Δ across strategies for Instances 3, 7, and 12

As illustrated in Figure 6, the relative ranking of strategies is consistent across all test cases: Model 2 achieves the lowest deviation in two instances and remains competitive even when outperformed in expectation by the random baseline, which is inherently variable. The bar chart further reinforces that the energy savings achieved are not due to randomness but rather to structured optimization.

5. Conclusion

This study introduces a bi-level optimization framework for heater placement in 2D manufacturing systems, achieving a balance between uniform heat distribution and energy efficiency. The first level ensures thermal uniformity by minimizing view factor deviations, while the second level minimizes active heaters to reduce energy consumption without compromising performance. Computational results demonstrate the framework's effectiveness across various scenarios, with an average reduction of 6% in heater usage while maintaining thermal uniformity.

The proposed approach contributes to the goals of Industry 4.0 by integrating advanced optimization and computational intelligence into the design of thermal systems, supporting smart production planning, energy efficiency, and sustainable manufacturing. Future work could extend this framework to dynamic control systems, incorporating real-time data analytics and automation for further optimization. Additionally, applying the methodology to other do- mains, such as additive manufacturing or semiconductor production, can lead to significant improvements in resource efficiency, product quality, and environmental sustainability, offering value to both industry and society.

References

Cheng, H.-C., Chung, I.-C., and Chen, W.-H. Response surface-based optimization approach for thermal placement design of chips in multiple-chip modules. IEEE Transactions on Components and Packaging Technologies, 32(3):531–541, 2009.

Cheng, H.-C., Tsai, Y.-H., Chen, K.-N., and Fang, J. Thermal placement optimization of multichip modules using a sequential metamodeling-based optimization approach. Applied Thermal Engineering, 30(17–18):2632–2642, 2010.

Daun, K. J., Howell, J. R., and Morton, D. Optimization of transient heater settings to provide spatially uniform heating in manufacturing processes involving radiant heating. Numerical Heat Transfer, Part A: Applications, 46(7):651–667, 2004.

Hachchadi, O., Tapsoba, G. R., Dery, P., Mechaqrane, A., Bourbonnais, M., Meloche, P., and Izquierdo, R. Experimental optimization of the heating element for a direct-coupled solar photovoltaic water heater. Solar Energy, 264:112037, 2023.

Jarny, Y. and Abou Khachfe, R. Numerical solution of 2-D nonlinear inverse heat conduction problems using finite-element techniques. Numerical Heat Transfer, Part B: Fundamentals, 37:45–67, 2000.

Liu, F.-B. A modified genetic algorithm for solving the inverse heat transfer problem of estimating plan heat source. International Journal of Heat and Mass Transfer, 51(15–16):3745–3752, 2008.

Raudensky, M., Woodbury, K., Kral, J., and Brezina, T. Genetic algorithm in solution of inverse heat conduction problems. Numerical Heat Transfer, Part B: Fundamentals, 28:293–306, 1995.

Biographies

Aybüke Ekşi is a Ph.D. candidate in the Industrial Engineering Department at Özyeğin University, Istanbul, Turkey. Her research focuses on operations research and mathematical optimization, with a particular interest in routing and logistics problems, including inventory and vehicle routing. Her work emphasizes the development of optimization models and algorithmic solution methods for real-world systems, including sustainable and energy-aware manufacturing systems. She is currently leading a comprehensive literature review article on Inventory Routing Problems, which is in the review process.

Altuğ Melik Başol is an Assistant Professor in the Mechanical Engineering Department at Özyeğin University, Istanbul, Turkey. He received his BSc and MSc degrees from Boğaziçi University, Istanbul, in Chemical and Mechanical Engineering, respectively. After receiving his Ph.D. degree from ETH Zurich in Switzerland in 2013, he continued to work as a post-doctoral researcher at the same university. His research focus is computational fluid dynamics, parallel programming, computing with GPU accelerators, numerical methods, gas and steam turbine aerodynamics, and heat transfer. During his research activities at ETH Zurich, he was involved in the research projects of the world's leading turbine and compressor manufacturers to improve their current design of turbomachinery, both in performance and reliability.

Milad Elyasi is an Assistant Professor in the Industrial Engineering Department at Özyeğin University, Istanbul, Turkey. He received his Ph.D. in Industrial Engineering, and his research interests include operations research, mathematical optimization, transportation and energy systems, and decision analytics. His work focuses on the development of optimization models and algorithms for complex industrial and energy-related problems, including sustainable manufacturing, energy-efficient system design, and large-scale optimization under uncertainty. He has published in international journals and conference proceedings and actively supervises graduate research in optimization and applied operations research.

Okan Örsan Özener has been a Professor in the Department of Industrial Engineering since 2008. He served as the Head of the Department of Industrial Engineering from 2012 to 2022 and as the Vice Dean of the Engineering Faculty from 2022 to 2024. Since January 2025, he has held the positions of Deputy Dean of the Faculty of Engineering and Deputy Director of the Graduate School of Engineering at Özyeğin University, Istanbul, Turkey. He received his B.Sc. (2001) and M.S. (2003) degrees in Industrial Engineering from Middle East Technical University. In 2006, he obtained his M.S. degree in Operations Research, and in 2008, his Ph.D. in Industrial and Systems Engineering from the Georgia Institute of Technology. He worked as a research assistant at Middle East Technical University from 2001 to 2003 and at Georgia Institute of Technology from 2003 to 2008. His research interests include data science, data-driven optimization, integer and combinatorial optimization, machine learning, non-cooperative and cooperative game theory, and supply chain management applications.